Journal of Anatomy

J. Anat. (2012) **221**, pp443–451 doi: 10.1111/j.1469-7580.2012.01559.x

Anatomical, architectural, and biochemical diversity of the murine forelimb muscles

Margie A. Mathewson,[1] Mark A. Chapman,[1] Eric R. Hentzen,[2,3] Jan Fridén[4] and Richard L. Lieber[1,2,3]

[1]*Department of Bioengineering, University of California, San Diego, La Jolla, CA, USA*
[2]*Department of Orthopedic Surgery, University of California, San Diego, La Jolla, CA, USA*
[3]*Department of Veterans Affairs Medical Center, San Diego, La Jolla, CA, USA*
[4]*Department of Hand Surgery, Sahlgrenska University Hospital, Gothenburg, Sweden*

Abstract

We characterized the architecture, fiber type, titin isoform distribution, and collagen content of 27 portions of 22 muscles in the murine forelimb. The mouse forelimb was different from the human arm in that it had the extensor digitorum lateralis muscle and no brachioradialis muscle. Architecturally, the mouse forelimb differed from humans with regard to load bearing, having a much larger contribution from extensors than flexors. In mice, the extensor : flexor PCSA ratio is 2.7, whereas in humans it is only 1.4. When the architectural difference index was calculated, similarities became especially apparent between flexors and extensors of the distal forelimb, as well as pronators. Discriminant analysis revealed that biochemical measures of collagen, titin, and myosin heavy chain were all strong between-species discriminators. In terms of composition, when compared with similar muscles in humans, mice had, on average, faster muscles with higher collagen content and larger titin isoforms. This report establishes the anatomical and biochemical properties of mouse forelimb muscles. Given the prevalence of this species in biological studies, these data will be invaluable for studying the biological basis of mouse muscle structure and function.

Key words: architecture; forelimb; model organism; mouse; muscle.

Introduction

Advances in human medical science often come from information gained through the use of animal models. To assess the strengths and weaknesses of animal data properly and to understand its significance, it is important to have a firm understanding of the unique features of an animal model and how those features relate to humans. For more than a century, functional morphologists have investigated the comparative anatomy of a variety of animals (Wood, 1867). The majority of studies in this field have performed bony anatomy comparisons across species. Studies on the comparative anatomy of muscle are less common and, recently, comparative muscles studies have identified notable differences between humans and other animals in areas such as the hand (Diogo et al. 2009). Recent studies of muscle in animals such as the dog or rat, (Sola et al. 1990; Eng et al. 2008) or comparisons of a single muscle across species (Guintard & Cossu, 2003) have suggested critical differences between humans and other mammals. Differences in gait between quadrupedal mammals and bipedal humans (Alexander, 2002; Steudel, 1996) may be related to many of these differences.

Because, now more than ever, human preclinical studies rely heavily on data from mouse models, it is useful to have comparative information regarding the composition and architecture of mouse muscle. While previous studies characterized a few individual mouse muscles (Hegarty & Hooper, 1971; Burkholder et al. 1994; Chleboun et al. 1997; Goulding et al. 1997) or determined a limited number of properties of an array of mouse muscles (Carry et al. 1993), a more complete understanding of architecture, fiber type, and composition for a wide array of muscles is beneficial. Tools such as MRI offer noninvasive ways to quantify certain aspects of small mouse muscles (Heemskerk et al. 2005) but these methods lack the fundamental data such as sarcomere length and serial sarcomere number. Thus, using MRI, there is no way to know if long fascicle lengths represent stretched sarcomeres from short fibers or if they actually represent a long string of sarcomeres. Additionally, biochemical composition data are still critical for accurate interpretation of new technologies. To date, no comprehensive study of the mouse forelimb has been undertaken to

Correspondence
Richard L. Lieber, Department of Orthopaedic Surgery, University of California San Diego and V.A. Medical Center, 9500 Gilman Drive, Mail Code 0863, La Jolla, CA 92093-0863, San Diego, USA. T: + 1 858 8221344; F: + 1 858 8223807; E: rlieber@ucsd.edu

Accepted for publication *6 August 2012*
Article published online *2 September 2012*

characterize its basic architectural and biochemical properties. Based on differences in size, mode of locomotion (quadrupedal vs. bipedal) (Clarke & Still, 1999; Winter, 1989) and the ability to manipulate using the digits, it is likely that significant differences would be present between the species. Muscles of a quadrupedal forelimb would be expected to be specialized for weight-bearing, since they would be critical in stabilization and force production during gait (Elftman, 1944; Macpherson, 1988; Johnson et al. 2008), whereas muscles of a biped might be expected to be adapted for manipulative capabilities (Dietz & Michel, 2009).

The purpose of this study was to compare the architectural and biochemical characteristics of the muscles of the mouse upper extremity to those of the human in order to draw conclusions about our ability to apply lessons learned from mouse models to our understanding of human disease. Based on the differences in locomotion and use of the limbs between species, we hypothesized that significant differences in architecture and biochemistry would be present between mouse and human forearms. Therefore, we characterized 27 portions of the 22 muscles of the mouse forelimb by measuring their architectural properties and determining their fiber type composition, collagen content, and titin isoforms.

Materials and methods

Tissue collection

All procedures were performed with approval of the University of California Animal Care and Use Committee. Six skeletally and sexually mature (Kilborn et al. 2002) male C57BL/6 mice (*Mus musculus*; Harlan Scientific, Indianapolis, IN, USA) between the ages of 8 and 11 weeks were euthanized by CO_2 inhalation followed by cervical dislocation, and the right and left forelimbs were removed. One limb from each mouse was pinned to a corkboard at a 90° elbow angle and fixed in 10% buffered formalin solution for 72 h. The sample was then placed in phosphate-buffered saline (PBS) for washing and storage until dissection. The contralateral limb from each mouse was immediately placed in cold mammalian Ringer's solution for further dissection. Muscles from that limb were dissected immediately and snap-frozen in liquid nitrogen (−196 °C). All fresh tissue dissection was completed within 4 h of euthanasia. Muscles were then maintained at −80 °C for storage until fiber analysis.

Architecture

Under a dissection microscope, individual muscles and their tendons were carefully dissected and placed in PBS for storage. Muscle identification was performed using a small animal anatomy text (Popesko et al. 1992) and previously published paper (Carry et al. 1993), along with guidance from two experienced hand surgeons. Twenty-two distinct muscles were found in the mouse forelimb, which corresponds to the human arm and forearm. Of these muscles, three had multiple heads, which were each dissected separately, yielding a total of 27 individually dissected muscles. These were: abductor pollicis longus (APL), anconeus (Ancon), biceps brachii-long head (Bic L), biceps brachii-short head (Bic S), brachialis (Brach), coracobrachialis (Coraco), dorso-epitrochlearis brachii (DEB), extensor carpi radialis brevis (ECRB), extensor carpi radialis longus (ECRL), extensor carpi ulnaris (ECU), extensor digiti quarti (EDQuart), extensor digiti quinti (EDQuint), extensor digitorum communis (EDC), extensor digitorum lateralis (EDL), extensor indicis proprius (EIP), flexor carpi radialis (FCR), flexor carpi ulnaris (FCU), flexor digitorum profundus-radial head (FDP R), flexor digitorum profundus-superficial head (FDP S), flexor digitorum profundus-ulnar head (FDP U), flexor digitorum superficialis (FDS), palmaris longus (PL), pronator quadratus (PQ), pronator teres (PT), triceps brachii-lateral head (Tri Lat), triceps brachii-long head (Tri Long), triceps brachii-medial head (Tri Med).

Using digital calipers under the microscope (accuracy, 0.01 mm), raw muscle length (L'_m), defined as the origin of the most proximal fibers to the insertion of the most distal fibers, was measured, and individual fibers were teased out to determine raw fiber length (L'_f). Muscles were gently blotted dry for mass measurement. Surface pennation angle was measured from enlarged muscle images using freely available software (IMAGEJ; U. S. National Institutes of Health, Bethesda, MD, USA). This computerized tool was chosen since direct measurement with a standard goniometer was deemed inaccurate due to the small size of these muscles. Tendon-to-tendon bundles were dissected from the muscle body and placed in weak sulfuric acid solution (15% v/v) for 30 min to weaken surrounding connective tissue and thus facilitate dissection. Small bundles of 10–20 individual fibers were then removed and placed on a glass slide for laser diffraction sarcomere length measurement. Raw sarcomere length (L'_s) was calculated using the first to first-order laser diffraction pattern as previously described (Lieber et al. 1984). Serial sarcomere number (S_n) and normalized fiber length (L_f) were calculated using the following formulas:

$$S_n = \frac{L'_f}{L'_s} \tag{1}$$

$$L_f = L'_f\left(\frac{2.4}{L'_s}\right) \tag{2}$$

where the value of 2.4 is optimal mouse sarcomere length based on the muscle length–tension relationship previously demonstrated (Hegarty & Hooper, 1971; Edman, 2005). This normalization method has been validated experimentally in mice (Felder et al. 2005).

To calculate an accurate physiological cross-sectional area (PCSA), the following formula was used (Powell et al. 1984):

$$PCSA = \frac{M \cdot \cos\theta}{\rho \cdot L_f} \tag{3}$$

where M is muscle mass (in grams), θ represents the average pennation angle of the muscle, and ρ is the density of muscle (1.056 g cm^{-3})(Ward and Lieber, 2005), and (L_f) is the normalized fiber length calculated above.

Architectural difference index calculation

The architectural difference index (ADI) was calculated (Lieber & Brown, 1992) to quantify the architectural difference between matched muscle pairs between species. For the calculations, the

architectural parameters that were the best discriminators were chosen for inclusion: fiber length, PCSA, muscle length, fiber length to muscle length ratio and muscle mass. The ADI equation previously developed:

$$\delta_{i,j} = \sqrt{\sum_{k=1}^{n} \left(\frac{P_{i,k} - P_{j,k}}{P_{\max,k} - P_{\min,k}} \right)^2} \quad (4)$$

was used, where $P_{i,k}$ and $P_{j,k}$ indicate the kth discriminating parameter for muscles i and j, respectively, and $P_{max,k}$ and $P_{min,k}$ are the maximum and minimum values for that parameter across the whole dataset. n is the number of total discriminating parameters (in this case, $n = 5$).

Myosin heavy chain and titin molecular weight determination

Muscle fiber type was estimated using myosin heavy chain composition as previously described (Talmadge and Roy, 1993). Snap-frozen muscles ($n = 3$ for each of 27 muscles) were weighed, crushed, and placed in sample buffer at a concentration of 125 μg mL^{-1}. Samples were loaded into SDS-PAGE gels, with 4% acrylamide stacking and 8% acrylamide resolving portions, and run at 4 °C at 10 mA constant current for 1 h followed by 275 V constant voltage for 16–22 h. The gels were trimmed and stained according to the BioRad Silver Stain Plus kit protocol (Bio-Rad, Hercules, CA), and bands were identified and quantified using densitometry (Quantity One; Bio-Rad).

Titin molecular weight was quantified using SDS-VAGE (Warren et al. 2003). A protein lysate was prepared as for fiber-type determination ($n = 3$ for each of 27 muscles) and loaded into 1% agarose gels held in place within the gel apparatus with a small 12.8% acrylamide plug. Gels were run at 15 mA for 5 h at 4 °C. Gels were stained according to the BioRad Silver Stain Plus kit protocol, and bands were identified and quantified using densitometry (Quantity One; Bio-Rad).

Collagen content measurement

Collagen content was determined using the hydroxyproline assay, which measures the content of hydroxyproline in a muscle sample (Stegemann and Stalder, 1967). Briefly, individual mouse muscles ($n = 3$ for each of 27 muscles) were placed in glass test tubes, immersed in six normal hydrochloric acid (HCl), and left to hydrolyze at 110 °C overnight. After tubes had cooled, methyl red was added to the tubes and the pH was adjusted using a series of sodium hydroxide and HCl additions in decreasing concentrations. Chloramine T solution was added to the tubes followed by p-diaminobenzaldehyde and tubes were incubated at 60 °C for 30 min. Samples were read at 550 and 558 nm and hydroxyproline concentrations were calculated based on the obtained standard curve. The measured value was converted to collagen concentration using the number of hydroxyproline residues in each collagen molecule (7.46).

Human data

Human data used for comparative purposes were obtained from previous studies (Lieber et al. 1990, 1992; Murray et al. 2000; Tirrell et al. 2012).

Statistical analysis

The statistics software SPSS was used for all statistical analyses. For flexor and extensor sarcomere length comparison, a two-tailed Student's t-test was performed with $P < 0.05$ set as the threshold for significance. One-way analysis of variance (ANOVA) was performed and *post hoc* comparisons were made with the Bonferroni multiple test correction with significance defined as $P < 0.05$. Discriminant analysis was performed in SPSS using normalized values for PCSA, mass, fiber length, and muscle length. None of the biochemical measures or pennation angle and fiber length to muscle length ratio was normalized.

Results

Mouse anatomy and architecture

A total of 162 muscles (27 muscles per mouse × six mice) were studied, with 54 muscles from the proximal forelimb and 108 from the portion distal to the elbow joint. Analysis of the mouse forelimb musculature showed several fundamental differences compared with humans. The mouse has an extensor digitorum lateralis (Fig. 1A), which is located next to the extensor digitorum communis and serves a similar function; an extensor digiti quarti (Fig. 1A), which is located near the extensor digiti quinti and extends the forth digit; and a dorsal epitrochlearis brachii (DEB)

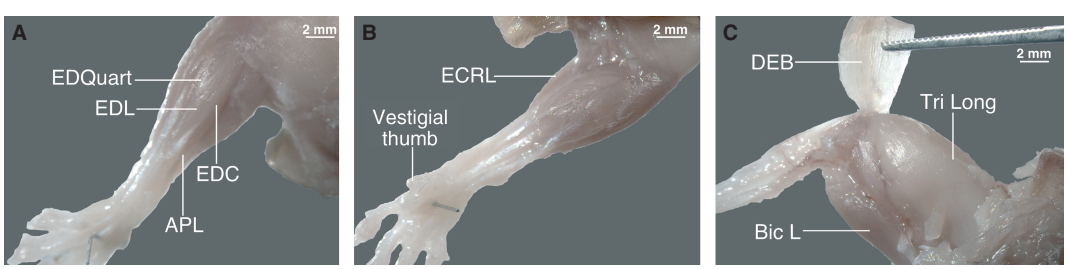

Fig. 1 (A) Extensor aspect of superficial mouse proximal and distal forelimb muscles. (B) Flexor aspect of mouse distal forelimb muscles. (C) Extensor aspect of mouse proximal forelimb muscles with the DEB muscle lifted to reveal the long head of the triceps. Images are all oriented distally (left) to proximally (right).

(Fig. 1C), which is a thin sheet of muscle that overlies the long head of the triceps. The DEB can actually be found in up to 17% of humans, but it is not a commonly recognized human muscle (Tubbs et al. 2006) and its functional significance is not clearly understood. In addition, the mouse is missing a brachioradialis muscle and has neither first digit flexors nor extensors (Fig. 1A,B), since the first digit appears to be a mainly vestigial, non-articulating appendage. The insertion site of the mouse biceps brachii varies between animals, with some inserting on the ulna, some on the radius, and some inserting on both. Of the muscles studied, the triceps brachii long head (Fig. 1C) was the clear architectural outlier with a mass and a PCSA that were an order of magnitude larger than any other muscle. Among the other muscles, all parameters were within the same range (Table 1).

To infer muscle function, it is useful to consider fiber length and PCSA (Fig. 2) since muscles with long fibers, which can contract quickly over a longer distance, are specialized for excursion whereas muscles with a large PCSA, and therefore many muscle fibers in parallel, are specialized for force production. Based on these data, muscles such as the FDS, FDP U and FCU would be expected to produce large forces with smaller excursions and slower contraction speeds, whereas the DEB, ECRL and ECRB all have comparatively higher excursion potential with their longer fibers and smaller PCSA. The Tri Long, an outlier on the graph, has both long fibers and a very large PCSA. In general, flexors of both the proximal and distal forelimb appear adapted for large force production, and extensors appear adapted for smaller force production but slightly greater excursion.

Collagen concentration

Mouse muscle collagen concentrations ranged from 11.4 μg mg^{-1} in the largest muscle (Tri Long) to 47.8 μg mg^{-1} in the small ulnar head of the FDP (Fig. 3). Although there appears to be a trend toward larger muscles having less collagen, the correlation between muscle mass and collagen content was insignificant ($P > 0.1$, $\beta = 0.84$). There was a significant difference between collagen concentration of the distal forelimb (corresponding to the forearm) and the proximal forelimb ($P < 0.001$) but con-

Table 1 Average architectural parameters for muscles of the mouse upper arm and forearm.

Muscle ($n = 6$)	Muscle length (mm)	Muscle mass (mg)	Fiber length (mm)	Pennation angle (deg.)	PCSA (mm^2)	L_f/L_m
Abductor pollicis longus*	7.73 ± 0.37	4.00 ± 0.24	1.98 ± 0.27	28.18 ± 1.16	1.90 ± 0.15	0.26 ± 0.04
Anconeus*	4.05 ± 0.16	1.08 ± 0.07	2.13 ± 0.22	24.65 ± 2.70	0.49 ± 0.05	0.52 ± 0.04
Biceps brachii long head	8.56 ± 0.36	16.12 ± 0.67	5.55 ± 0.24	21.68 ± 1.24	2.60 ± 0.09	0.66 ± 0.05
Biceps brachii short head	9.50 ± 0.37	18.85 ± 2.62	5.98 ± 0.37	28.27 ± 1.26	2.80 ± 0.51	0.63 ± 0.04
Brachialis	5.53 ± 0.51	3.42 ± 0.82	4.10 ± 0.23	9.89 ± 2.30	0.83 ± 0.2	0.77 ± 0.07
Coracobrachialis	8.39 ± 0.24	4.02 ± 0.47	4.30 ± 0.58	13.85 ± 1.46	0.95 ± 0.13	0.52 ± 0.07
Dorso-epitrochlearis brachii*	6.42 ± 0.15	6.97 ± 0.34	5.49 ± 0.22	31.56 ± 4.06	1.04 ± 0.06	0.85 ± 0.03
Extensor carpi radialis brevis*	7.67 ± 0.28	7.45 ± 0.31	6.04 ± 0.44	29.49 ± 1.73	1.17 ± 0.11	0.79 ± 0.06
Extensor carpi radialis longus*	7.76 ± 0.35	7.20 ± 0.46	5.60 ± 0.47	26.40 ± 1.38	1.26 ± 0.15	0.73 ± 0.07
Extensor carpi ulnaris*	6.49 ± 0.24	4.75 ± 0.23	2.74 ± 0.21	20.80 ± 1.28	1.72 ± 0.16	0.42 ± 0.03
Extensor digiti quarti*	6.16 ± 0.24	0.88 ± 0.17	3.60 ± 0.40	15.74 ± 1.82	0.24 ± 0.04	0.58 ± 0.05
Extensor digiti quinti*	5.96 ± 0.25	1.15 ± 0.15	4.06 ± 0.23	14.37 ± 1.50	0.29 ± 0.04	0.68 ± 0.04
Extensor digitorum communis*	7.81 ± 0.47	2.78 ± 0.37	3.84 ± 0.16	18.56 ± 1.90	0.67 ± 0.08	0.50 ± 0.04
Extensor digitorum lateralis*	6.22 ± 0.17	1.80 ± 0.23	4.38 ± 0.43	22.81 ± 1.78	0.41 ± 0.06	0.71 ± 0.07
Extensor indicis proprius*	5.48 ± 0.30	0.75 ± 0.11	3.78 ± 0.54	19.00 ± 1.33	0.22 ± 0.04	0.71 ± 0.12
Flexor carpi radialis	7.52 ± 0.29	5.13 ± 0.24	3.67 ± 0.33	15.02 ± 0.87	1.27 ± 0.10	0.49 ± 0.03
Flexor carpi ulnaris	8.19 ± 0.15	9.77 ± 0.28	3.80 ± 0.42	20.95 ± 1.51	2.29 ± 0.27	0.46 ± 0.05
Flexor digitorum profundus radial head	6.14 ± 0.14	2.55 ± 0.21	4.06 ± 0.27	13.98 ± 1.61	0.64 ± 0.10	0.66 ± 0.05
Flexor digitorum profundus superficial head	7.80 ± 0.09	5.33 ± 0.22	3.22 ± 0.18	18.14 ± 1.63	1.59 ± 0.15	0.41 ± 0.02
Flexor digitorum profundus Ulnar head	8.17 ± 0.49	10.85 ± 0.29	3.40 ± 0.24	18.81 ± 1.62	2.96 ± 0.29	0.43 ± 0.05
Flexor digitorum superficialis	9.99 ± 0.17	7.57 ± 0.19	2.50 ± 0.31	18.96 ± 2.41	2.84 ± 0.31	0.25 ± 0.03
Palmaris longus	5.96 ± 0.44	3.88 ± 0.34	3.62 ± 0.18	24.65 ± 2.02	0.91 ± 0.07	0.63 ± 0.05
Pronator quadratus	4.35 ± 0.87	0.93 ± 0.21	0.82 ± 0.05	79.47 ± 0.53	0.21 ± 0.05	0.30 ± 0.13
Pronator teres	6.63 ± 0.14	4.77 ± 0.19	2.56 ± 0.33	26.17 ± 1.92	1.84 ± 0.25	0.38 ± 0.05
Triceps brachii lateral head*	9.37 ± 0.51	17.50 ± 1.30	6.29 ± 0.35	23.41 ± 2.01	2.37 ± 0.17	0.68 ± 0.05
Triceps brachii long head*	10.93 ± 0.13	103.65 ± 3.53	5.32 ± 0.54	41.88 ± 1.33	15.49 ± 3.37	0.49 ± 0.05
Triceps brachii medial head*	8.19 ± 0.34	9.20 ± 1.95	5.10 ± 0.25	30.33 ± 3.67	1.50 ± 0.39	0.63 ± 0.06

L_f, fiber length normalized to mouse optimal sarcomere length (2.4 μm); L_m, muscle length normalized in the same way.
Values are means ± SEM.
*Anti-gravity muscle.

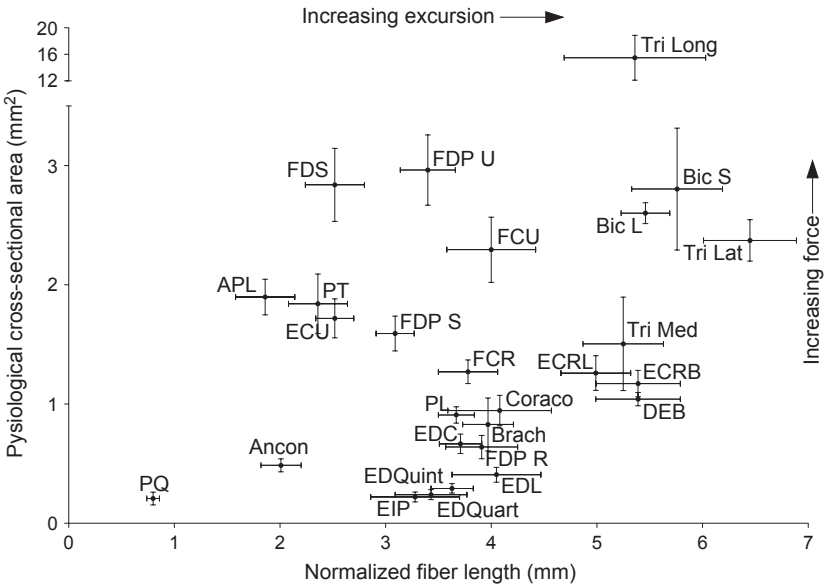

Fig. 2 Mouse PCSA vs. normalized fiber length (to a sarcomere length of 2.4 μm) plotted to illustrate relative muscle forces and excursions. Tri Long is an outlier in PCSA, so the vertical axis has been broken to allow other muscles to be clearly viewed. Data are plotted as mean ± SEM (n = 6).

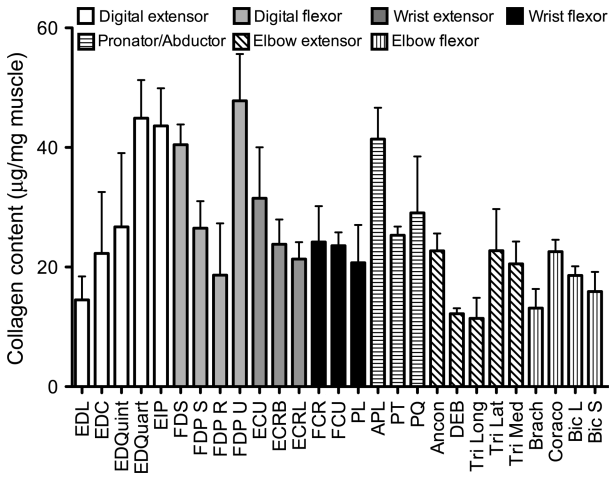

Fig. 3 Collagen content of mouse forelimb muscles. Data are expressed as μg collagen per mg wet weight of frozen muscle. Data are plotted as mean ± SEM (n = 3).

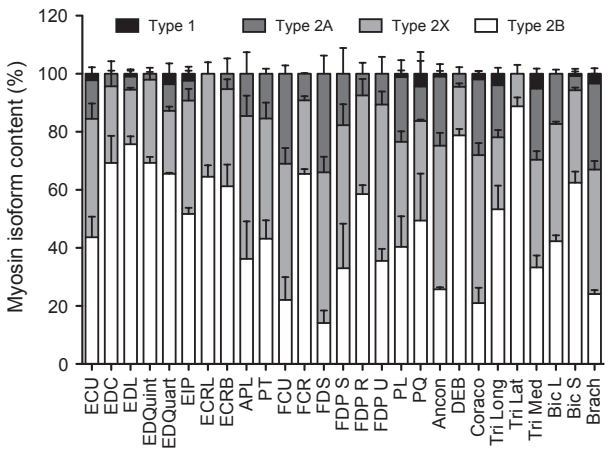

Fig. 4 Myosin heavy chain isoform percentages of mouse forelimb muscles. Data are plotted as mean ± SEM (n = 3).

centration differences between flexors and extensors or digital muscles and wrist muscles were not significant ($P > 0.4$).

Myosin heavy chain

Myosin heavy chain type 2B, the fastest isoform, dominated the mouse MHC profile. The combination of types 2X and 2B made up ~ 85% of the total myosin in the mouse forelimb. Myosin type 2A was detected in all muscles but the ECRL and the lateral head of the triceps (Fig. 4). Myosin type 1 was detected in only 12 of the muscles studied, and it constituted < 6% in each of these muscles. Overall, these data demonstrate that mouse muscle is very 'fast', as it is predominately composed of the fastest MHC isoforms.

Titin composition

All mouse titin isoforms ranged from 3350 to 3750 kDa (Fig. 5), which was similar to values reported in previous studies of mouse leg muscles (Ottenheijm et al. 2009) and similar to the range reported for rabbit muscle (Prado et al. 2005). Titin isoform size was not statistically significantly different ($P > 0.25$, $\beta = 0.89$) among muscles groups when they were classified as distal forelimb extensors or flexors or proximal forelimb flexors or extensors. Distal forelimb flexor titin isoforms showed a slight trend toward being longer than those of other groups, but *post hoc* testing

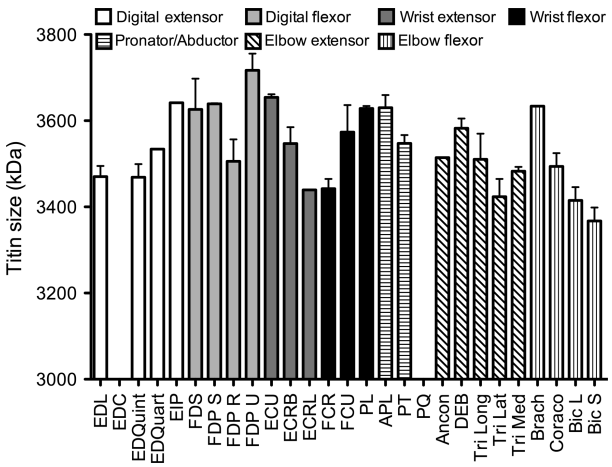

Fig. 5 Titin isoform size variation in mouse forelimb muscles. Data were not obtained from the PQ and EDC, and muscles with no error bar show data from a single sample. Data are plotted as mean ± SEM (n = 3).

with Bonferroni corrections showed that the trend was not significant ($P > 0.5$).

Discussion

The purpose of this study was to determine the extent to which the basic anatomy of the mouse forelimb is similar to that of the human arm and to define its biochemical composition. The distal forelimb muscles that correspond to human forearm muscles are in similar locations and appear to have similar functions. Using previously collected human data (Lieber et al. 1990; Lieber & Brown, 1992; Murray et al. 2000), we compared mouse data with that of humans. When functional indicators such as the PCSA vs. fiber length graph shown previously are used, similarities between mouse distal forelimbs and human forearms become apparent. We created a graph of normalized human and mouse PCSA and fiber length (Fig. 6) in which the muscles of the distal and proximal forelimb of each species were normalized to the other muscles in that group (i.e. distal forelimb muscles from each species were normalized using the average of all distal forelimb muscles for that species) to facilitate comparison. It is clear from the plot that, although not identical, distal forelimb extensors muscles are functionally similar between the two species. Proximal forelimb muscles and several of the distal flexors, on the other hand, show drastic differences between the two species. These dissimilarities are not surprising considering differences in locomotion between the two species. The function of the proximal forelimb, especially, varies considerably between a bipedal and quadrupedal creature (Miller, 1932). Digital flexors of humans appear to be more specialized for excursion than those of mice, which might be expected of a creature requiring dexterous finger movements. Digital flexors of mice, as compared with those of humans, on the other hand, appear adapted for force production, as might be expected in a species that primarily uses its forelimb for weight-bearing (Hamrick, 1996; Clarke & Still, 1999; Courtine et al. 2007).

To compare quantitatively between different species' muscles, the architectural difference index (ADI) was calculated (Lieber & Brown, 1992). This number combines calculated differences between five selected architectural variables (L_{fn}, L_{mn}, mass, PCSA, and L_{fn} : L_{mn} ratio) to create a single number that allows normalization of muscles so that they can be compared across groups and species. The ADI (Fig. 7) shows more than a fivefold difference between the most and least similar muscles of the two species. High similarity, (defined in this study as an ADI < 0.5) was seen in the ECRL, FCR, PL, EDC, EIP, PQ, and PT. An ADI > 2, as seen in the muscles of the triceps, indicates a large difference

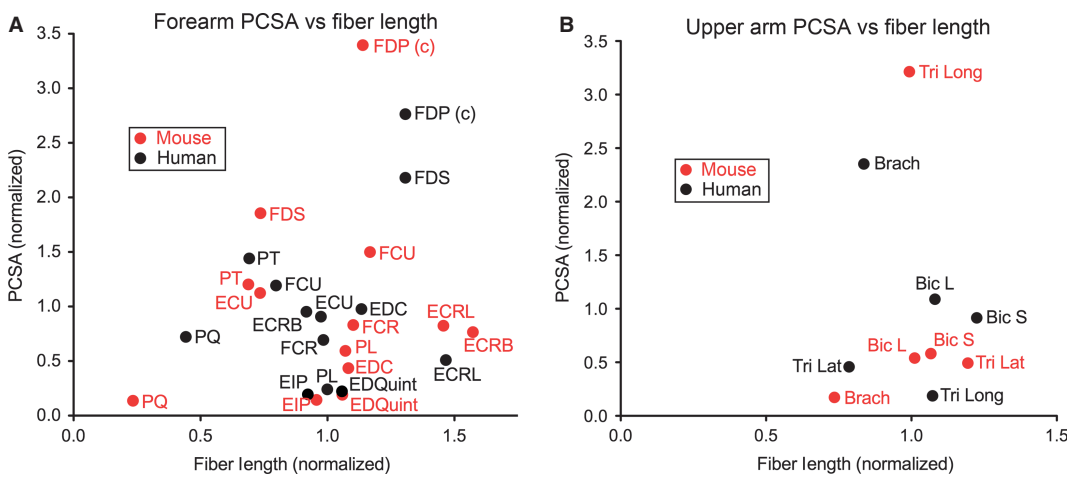

Fig. 6 Plot of PCSA vs. fiber length for the distal (A) and proximal forelimb muscles (B) of the human and mouse. Data for each species have been normalized to the average of all muscles of that species on the graph (distal normalized to distal muscles and proximal to proximal). A (c) after a muscle name indicates that it is the combined value of all heads of the muscle. Human data were obtained from previously published values. (Lieber et al. 1990, 1992; Murray et al. 2000).

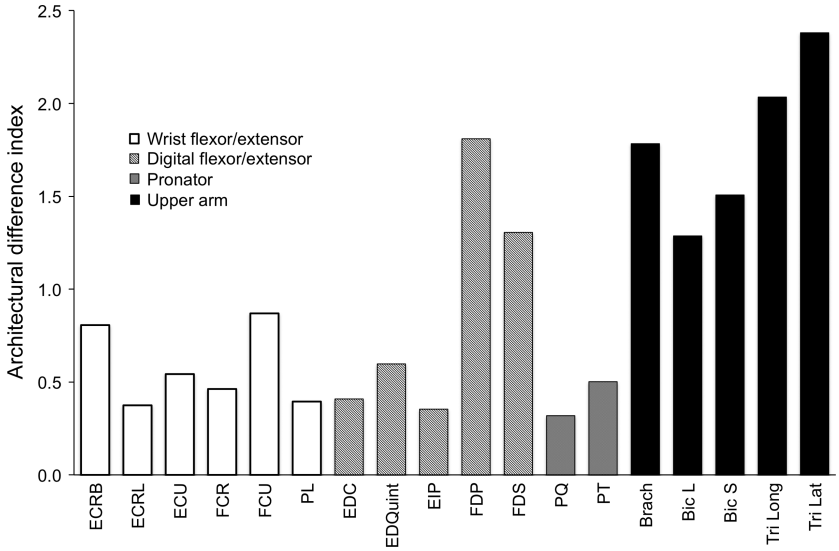

Fig. 7 Architectural difference index (ADI) of select human and mouse muscles shows relative similarity between the same muscle in mice and humans based on architectural parameters. Lower ADI indicates greater similarity.

between muscles. All muscles of the distal forelimb besides the digital flexors had an ADI < 1, suggesting similarity to humans.

There are distinct muscular differences between the human and mouse forelimb. Since the mouse first digit is small and does not appear to be jointed, first digit muscles found in the human that allow flexion and extension are unnecessary in the mouse. The only first digit muscle found in the mouse forelimb was the APL, which appears to contribute to movement of the whole paw. Another important human muscle, the brachioradialis, is not present in the mouse. The ECRL and ECRB muscle bellies are shifted anteriorly compared with humans, but they still extend the wrist and attach to the paw in a location corresponding to their location in the human hand. In the proximal portion of the forelimb, the long head of the mouse triceps contributes a much greater percentage of mass than human triceps do. Because both biceps and triceps contribute to weight-bearing and stabilization in quadrupeds such as mice (Williams et al. 2008, Fuentes et al. 1998), but only biceps serve an antigravity function in humans (Monster et al. 1978), it is not surprising that the mouse triceps was larger and adapted more for force-production compared with the human triceps. Since the long head of the triceps crosses both the elbow and shoulder joint, it contributes even more significantly to quadrupedal locomotion than the other heads of the triceps. Many adaptations, such as the lack of first digit muscles in the mouse, are likely due to this difference in forelimb specialization: weight-bearing in mice and manipulation in humans.

At the biochemical level, mouse muscles are dissimilar from human muscles (Fig. 8). Mouse muscles have a completely different myosin heavy chain (MHC) distribution, and therefore a different fiber type distribution, compared to human muscles (Tirrell et al. 2012) (Fig. 8A). Compared with human data, mice had about a third as much type IIA myosin and nearly twice as much type IIX as humans (Tirrell et al. 2012). Type IIB MHC, which is the major component of the mouse muscles studied, is not expressed in human muscles (Smerdu et al. 1994). Because this major component

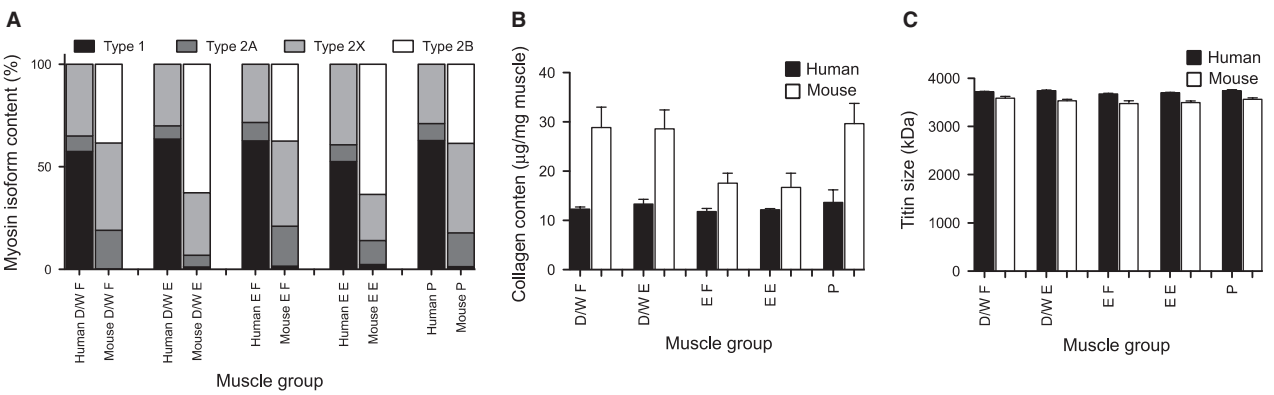

Fig. 8 Biochemical comparisons between human and mice muscle groups (D/W F , digital and wrist flexors; D/W E, digital and wrist extensors; E F, elbow flexors; E E , elbow extensors; P, pronators) show large differences in myosin (A) and collagen (B), but smaller differences in titin isoform composition (C). Human data from Tirrell et al. (2012).

of mouse myosin is the fastest myosin isoform, and because type IIX is also fast, mouse muscles would be expected to be much faster contracting compared with human muscles. Previous studies suggest that smaller mammals have faster muscles in general, with mouse muscle V_{max} ranging from 6 to 20.6 L s^{-1} and human V_{max} from 0.35 to 3.68 L s^{-1} (Medler, 2002; Pellegrino et al. 2003). A small, short-limbed mammal would have to take more rapid strides to maintain the same speed as a larger mammal with longer limbs (Heglund & Taylor, 1988), as in the case of a mouse escaping a predator. Because of this, a fiber type distribution shifted toward myosin isoforms with higher shortening velocity makes evolutionary and functional sense. Whereas the slowest isoform, type I myosin, is almost completely absent in mouse forelimb muscles, human muscles express high levels of myosin isoform I (Happak et al. 1988; Tirrell et al. 2012).

The mouse titin isoforms are in the same size range as published figures for human titin, 3300–3700 kDa (Maruyama, 1997) (Fig. 8C) but mouse values were found to be, on average, ~ 180 kDa smaller. Titin molecular weights were more different from those of humans in the proximal portion of the forelimb than in the distal (Tirrell et al. 2012).

The average collagen concentration in the mouse forelimb muscles, 25.4 μg mg^{-1}, is double that of human muscles (Fig. 8B) from a similar set of arm muscles recently measured from cadaveric specimens (Tirrell et al. 2012). It has been noted previously that smaller mammals store less elastic energy in their tendons (Biewener et al. 1981; Pollock & Shadwick, 1994) and it is possible that the increased collagen seen in the mouse muscles serves a compensatory role, allowing greater muscle tissue elastic energy storage despite small muscle forces preventing large stores in tendons. In the mouse muscles tested here, smaller muscles tended to have higher collagen concentrations. There is a possibility that this was due to the very small size of the muscle samples, some of which weighed < 1 mg, and the associated difficulty of completely removing all tendon. It is also possible that the surface area to volume ratio of these small muscles was such that the surrounding connective tissue made a much larger contribution than it would in a large muscle.

Overall, this study shows several significant anatomical differences between mouse and human forelimb, and warns against the use of proximal forelimb muscles for accurate architectural representations of human arm muscles. Some mouse muscles may still provide good representations of human muscles; for example, pronators, digital extensors, and select wrist muscles show high overall architectural similarity to their human counterparts both with regard to excursion vs. force production and ADI. However, digital flexors and all muscles of the proximal forelimb show little similarity to those of humans. Obviously, some muscles of great interest in human disorders, such as the brachioradialis, cannot be modeled in mice, since they are absent. At the biochemical level, mouse muscles show much less similarity to their human counterparts than they do architecturally. In view of the many differences between mouse and human muscles, it is clear that care must be taken when choosing acceptable mouse muscles for studies of corresponding human disease.

Acknowledgements

The authors acknowledge the expert advice of Dr. Ki Lee and Tim Tirrell. Technical assistance was provided by Mary Esparza and Evie Lin. The authors have no competing interests to disclose.

Funding

This work was supported by the Rehabilitation Research and Development Service of the Department of Veterans Affairs, NIH grant HD050837, and National Science Foundation Graduate Research Fellowships to M.M. and M.C.

Author contributions

M.M. and M.C. contributed to acquisition, analysis, and interpretation of data, drafting and revising the article, and approving the final version. E.H. and J.F. contributed to interpretation of data, critically revising article, and approving the final version. R.L. contributed to conception and design of the study, analysis and interpretation of data, drafting and critically revising the article, and approving the final version.

References

Alexander RM (2002) Stability and manoeuvrability of terrestrial vertebrates. *Integr Comp Biol* **42**, 158–164.

Biewener A, Alexander RM, Heglund NC (1981) Elastic energy storage in the hopping of kangaroo rats (*Dipodomys spectabilis*). *J Zool* **195**, 369383.

Burkholder TJ, Fingado B, Baron S, et al. (1994) Relationship between muscle fiber types and sizes and muscle architectural properties in the mouse hindlimb. *J Morphol* **221**, 177–190.

Carry MR, Horan SE, Reed SM, et al. (1993) Structure, innervation, and age-associated changes of mouse forearm muscles. *Anat Rec* **237**, 345–357.

Chleboun GS, Patel TJ, Lieber RL (1997) Skeletal muscle architecture and fiber-type distribution with the multiple bellies of the mouse extensor digitorum longus muscle. *Acta Anat (Basel)* **159**, 147–154.

Clarke KA, Still J (1999) Gait analysis in the mouse. *Physiol Behav* **66**, 723–729.

Courtine G, Bunge MB, Fawcett JW, et al. (2007) Can experiments in nonhuman primates expedite the translation of treatments for spinal cord injury in humans? *Nat Med* **13**, 561–566.

Dietz V, Michel J (2009) Human bipeds use quadrupedal coordination during locomotion. *Ann N Y Acad Sci* **1164**, 97–103.

Diogo R, Abdala V, Aziz MA, et al. (2009) From fish to modern humans – comparative anatomy, homologies and evolution of the pectoral and forelimb musculature. *J Anat* **214**, 694–716.

Edman KAP (2005) Contractile properties of mouse single muscle fibers, a comparison with amphibian muscle fibers. *J Exp Biol* **208**, 1905–1913.

Elftman H (1944) The bipedal walking of the chimpanzee. *J Mammal* **25**, 67–71.

Eng CM, Smallwood LH, Rainiero MP, et al. (2008) Scaling of muscle architecture and fiber types in the rat hindlimb. *J Exp Biol* **211**, 2336–2345.

Felder A, Ward SR, Lieber RL (2005) Sarcomere length measurement permits high resolution normalization of muscle fiber length in architectural studies. *J Exp Biol* **208**, 3275–3279.

Fuentes I, Cobos AR, Segade LAG (1998) Muscle fibre types and their distribution in the biceps and triceps brachii of the rat and rabbit. *J Anat* **192**, 203–210.

Goulding D, Bullard B, Gautel M (1997) A survey of in situ sarcomere extension in mouse skeletal muscle. *J Muscle Res Cell Motil* **18**, 465–472.

Guintard C, Cossu F (2003) Comparative anatomy of M-extensor carpi radialis in 9 species of domestic mammals and in man. *Rev Med Vet* **154**, 115–119.

Hamrick MW (1996) Locomotor adaptations reflected in the wrist joints of early tertiary primates (Adapiformes). *Am J Phys Anthropol* **100**, 585–604.

Happak W, Burggasser G, Gruber H (1988) Histochemical characteristics of human mimic muscles. *J Neurol Sci* **83**, 25–35.

Heemskerk AM, Strijkers GJ, Vilanova A, et al. (2005) Determination of mouse skeletal muscle architecture using three-dimensional diffusion tensor imaging. *Magn Reson Med* **53**, 1333–1340.

Hegarty PVJ, Hooper AC (1971) Sarcomere length and fibre diameter distributions in four different mouse skeletal muscles. *J Anat* **110**, 249–257.

Heglund NC, Taylor CR (1988) Speed, stride frequency and energy cost per stride: how do they change with body size and gait? *J Exp Biol* **138**, 301–318.

Johnson WL, Jindrich DL, Roy RR, et al. (2008) A three-dimensional model of the rat hindlimb: musculoskeletal geometry and muscle moment arms. *J Biomech* **41**, 610–619.

Kilborn SH, Trudel G, Uhthoff H (2002) Review of growth plate closure compared with age at sexual maturity and lifespan in laboratory animals. *J Am Assoc Lab Anim Sci* **41**, 21–26.

Lieber RL, Brown CG (1992) Quantitative method for comparison of skeletal muscle architectural properties. *J Biomech* **25**, 557–560.

Lieber RL, Yeh Y, Baskin RJ (1984) Sarcomere length determination using laser diffraction. Effect of beam and fiber diameter. *Biophys J* **45**, 1007–1016.

Lieber RL, Fazeli BM, Botte MJ (1990) Architecture of selected wrist flexor and extensor muscles. *J Hand Surg Am* **15**, 244–250.

Lieber RL, Jacobson MD, Fazeli BM, et al. (1992) Architecture of selected muscles of the arm and forearm: anatomy and implications for tendon transfer. *J Hand Surg Am* **17**, 787–798.

Macpherson JM (1988) Strategies that simplify the control of quadrupedal stance. II. Electromyographic activity. *J Neurophysiol* **60**, 218–231.

Maruyama K (1997) Connectin/titin, giant elastic protein of muscle. *FASEB J* **11**, 341–345.

Medler S (2002) Comparative trends in shortening velocity and force production in skeletal muscles. *Am J Physiol Regul Integr Comp Physiol* **283**, R368–R378.

Miller RA (1932) Evolution of the peotoral girdle and fore limb in the Primates. *Am J Phys Anthropol* **17**, 1–56.

Monster A, Chan H, O'Connor D (1978) Activity patterns of human skeletal muscles: relation to muscle fiber type composition. *Science* **200**, 314–317.

Murray WM, Buchanan TS, Delp SL (2000) The isometric functional capacity of muscles that cross the elbow. *J Biomech* **33**, 943–952.

Ottenheijm CAC, Knottnerus AM, Buck D, et al. (2009) Tuning passive mechanics through differential splicing of titin during skeletal muscle development. *Biophys J* **97**, 2277–2286.

Pellegrino MA, Canepari M, Rossi R, et al. (2003) Orthologous myosin isoforms and scaling of shortening velocity with body size in mouse, rat, rabbit and human muscles. *J Physiol* **546**, 677–689.

Pollock CM, Shadwick RE (1994) Allometry of muscle, tendon, and elastic energy storage capacity in mammals. *Am J Physiol* **266**, R1022–R1031.

Popesko P, Rajtova V, Horak J (1992) *A Color Atlas of Anatomy of Small Laboratory Animals*. Prescott, AZ: Wolfe Publishing Ltd.

Powell PL, Roy RR, Kanim P, et al. (1984) Predictability of skeletal muscle tension from architectural determinations in guinea pig hindlimbs. *J Appl Physiol* **57**, 1715–1721.

Prado LG, Makarenko I, Andresen C, et al. (2005) Isoform diversity of giant proteins in relation to passive and active contractile properties of rabbit skeletal muscles. *J Gen Physiol* **126**, 461–480.

Smerdu V, Karsch-Mizrachi I, Campione M, et al. (1994) Type IIx myosin heavy chain transcripts are expressed in type IIb fibers of human skeletal muscle. *Am J Physiol* **267**, C1723–C1728.

Sola OM, Haines LC, Kakulas BA, et al. (1990) Comparative anatomy and histochemistry of human and canine latissimus-dorsi muscle. *J Heart Transplant* **9**, 151–159.

Stegemann H, Stalder K (1967) Determination of hydroxyproline. *Clin Chim Acta* **18**, 267–273.

Steudel K (1996) Limb morphology, bipedal gait, and the energetics of hominid locomotion. *Am J Phys Anthropol* **99**, 345–355.

Talmadge RJ, Roy RR (1993) Electrophoretic separation of rat skeletal muscle myosin heavy-chain isoforms. *J Appl Physiol* **75**, 2337–2340.

Tirrell TF, Cook MS, Carr JA, et al. (2012) Human skeletal muscle biochemical diversity. *J Exp Biol* **215**, 2551–2559.

Tubbs RS, Salter EG, Oakes WJ (2006) Triceps brachii muscle demonstrating a fourth head. *Clin Anat* **19**, 657–660.

Ward SR, Lieber RL (2005) Density and hydration of fresh and fixed human skeletal muscle. *J Biomech* **38**, 2317–2320.

Warren CM, Krzesinski PR, Greaser ML (2003) Vertical agarose gel electrophoresis and electroblotting of high-molecular-weight proteins. *Electrophoresis* **24**, 1695–1702.

Williams SB, Wilson AM, Daynes J, et al. (2008) Functional anatomy and muscle moment arms of the thoracic limb of an elite sprinting athlete: the racing greyhound (*Canis familiaris*). *J Anat* **213**, 373–382.

Winter DA (1989) Biomechanics of normal and pathological gait – implications for understanding human locomotor control. *J Mot Behav* **21**, 337–355.

Wood J (1867) On human muscular variations and their relation to comparative anatomy. *J Anat Physiol* **1**, 44–59.